Experimental validation of BEAMS3D and application to ASDEX Upgrade

D. Kulla[1,2], S. Lazerson[1], A. Kappatou[2],
H. Zohm[2], R. C. Wolf[1], and the ASDEX Upgrade Team*
[1] *Max-Planck-Institut für Plasmaphysik, Wendelsteinstr. 1 Greifswald, DE 17491*
[2] *Max-Planck-Institut für Plasmaphysik, Boltzmannstr. 2, Garching bei München, DE 85748*
** See author list of U. Stroth et al., 2022 Nucl. Fusion 62, 042006*

We present progress on experimental validation of the BEAMS3D [1] Monte-Carlo code using the fast-ion D-α (FIDA) diagnostic at ASDEX Upgrade (AUG) and FIDASIM [2]. The validated code is then applied to simulate the effects of a three-dimensional magnetic perturbation on the fast ion distribution and measured FIDA signals.

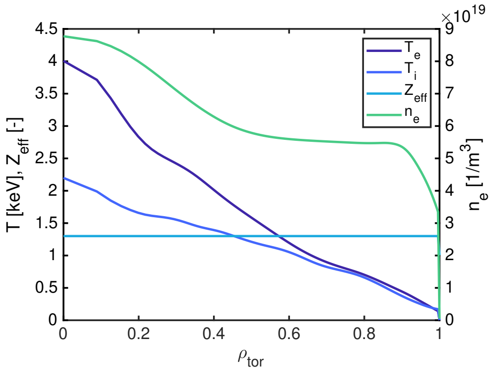

Figure 1: Profiles of AUG shot #38581@5.65 s used for input.

For magnetic confinement fusion, understanding the dynamics of fast ion confinement is crucial to effectively achieve plasma heating and to mitigate potential damage to the first wall of a future fusion reactor. Tokamaks are susceptible to increased fast ion transport as a consequence of magnetic perturbations: these can be either externally induced by special coils or generated internally by the plasma itself. In contrast, stellarators, which inherently have three-dimensional magnetic fields, typically exhibit decreased fast ion confinement which needs to be optimized to suitable levels for a reactor. These effects on confinement behaviour underscore the need for robust, validated computational tools to study and predict fast ion dynamics in different magnetic configurations.

BEAMS3D is a Monte-Carlo code that offers simulation capabilities to obtain the steady-state fast ion distribution in both axisymmetric and 3D fields. Using a newly developed interface for EQDSK equilibria, its capability in axisymmetric tokamak plasmas is similar to that of the proven NUBEAM code (part of the TRANSP suite) [3]. As such, we perform verification and validation of the two codes simultaneously. AUG shot #38581 is chosen for this activity, as it features long phases of on- and off-axis neutral beam heating. We will show results only for the off-axis phase for brevity, since this configuration is more challenging for the model. The kinetic profiles of AUG shot #38581 at 5.56 s used as input for the codes are visible in fig. 1. Both codes are run with about 50k markers for the simulations. A principal difference of BEAMS3D

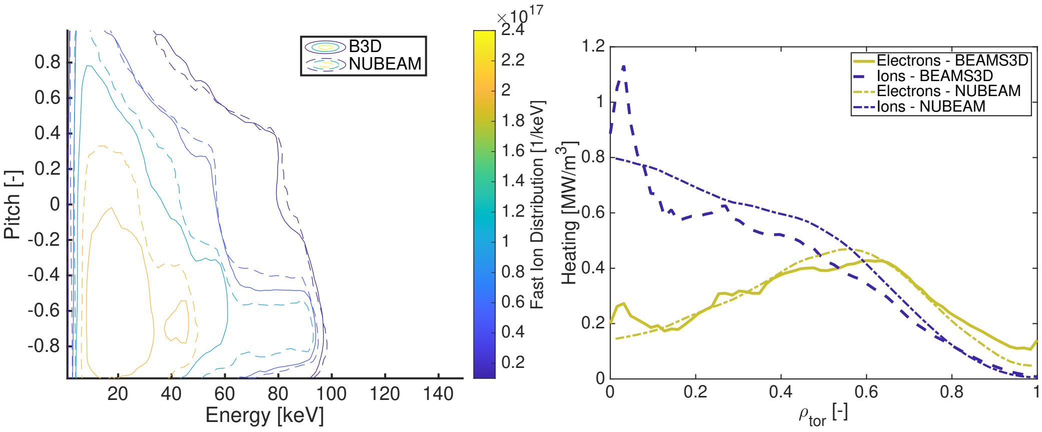

Figure 2: Left: Comparison of the energy-pitch distribution, integrated over all spatial coordinates. Right: Radial profiles of electron and ion heating obtained by both codes.

compared to NUBEAM is the omission of the plasma rotation. However, we have included this effect through the neoclassical radial electric field into the BEAMS3D calculation. This acts as a potential well for the orbiting particles and tilts otherwise constant energy contours with respect to the pitch ($\lambda = v_{||}/v$, the ratio of the velocity parallel to the magnetic field to the total velocity).

The match between BEAMS3D and NUBEAM in the energy-pitch distribution is visible in fig. 2. Also visible in this figure are the calculated radial heating profiles by both codes for fast-ion heating to the thermal electrons and ions. The profiles match well considering the BEAMS3D profile has a much higher resolution. The slight mismatch in the core region is attributed to minor differences in the formulation of the slowing down operators. A spike at r/a=1 is visible in the electron channel, caused by particles orbiting outside the plasma.

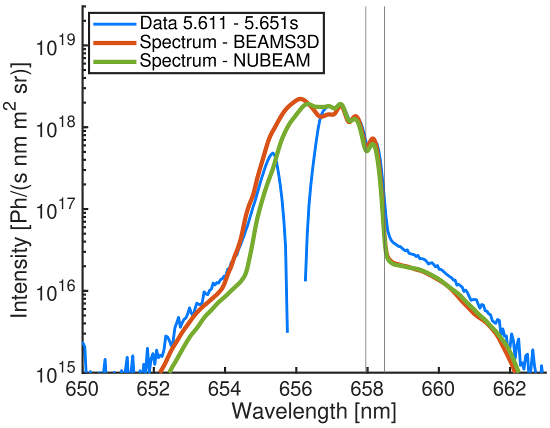

Figure 3: FIDA spectrum of shot #38581 with forward-modelled spectra using BEAMS3D or NUBEAM as well as FIDASIM.

Based on the fast ion distribution obtained by both codes, we use FIDASIM to obtain synthetic spectra which can be compared to those measured by the FIDA diagnostic. On the BEAMS3D side, this leveraged a new interface developed during this project, as well as changes to the calculation of the distribution function. The comparison of the measured and simulated spectra is visible in fig. 3. General agreement between all three spectra can be observed. To prevent over-saturation, a wire blocks the D-α line around 656.1 nm in the measures spectrum. The part of the spectrum dominated by beam emission (excited neutrals emitting light) is marked by vertical lines. Here, a small shift in wavelength between the measurement and the simulations can be seen. This phenomenon is currently being carefully investigated to conclude the validation. The spectrum to the right of the beam emission is dominated by charge exchange of fast ions with the beam neutrals, the actual FIDA emission. The magnitude is a bit low even considering the wavelength shift, but the shape of the spectrum is well represented in the simulation.

Using the validated code, three-dimensional magnetic perturbations can be investigated. The top panel of fig. 4 shows time traces of AUG shot #41098. In this shot, a neoclassical tearing mode appears shortly before the programmed end. It is stabilized through ECRH heating, but grows larger and eventually locks to the external error field at 7.3 s. The slowing down and eventual locking is clearly visible in the T_e and v_{rot} traces, and temperature flattening can also be observed in the profiles (not shown). The RMP coils were inactive for this shot. Towards the end of the discharge, the ECRH is turned off shortly after the mode locks, and impurities start to accumulate, raising Z_{eff}. The bottom panel shows the integral of the FIDA part of the spectrum (660-661 nm, corresponding to passing particles above 30 keV) normalized to that dominated by the beam emission. No large impact of the locking mode on the fast ion measurements can be seen here, and fast ion levels are comparable to the rest of the shot when conditions are similar. In contrast, an MHD event appears as the impurity accumulation peaks before 7.4 s, which causes a large and sudden decrease in fast ion content simultaneous to the decrease in density and W_{mhd}.

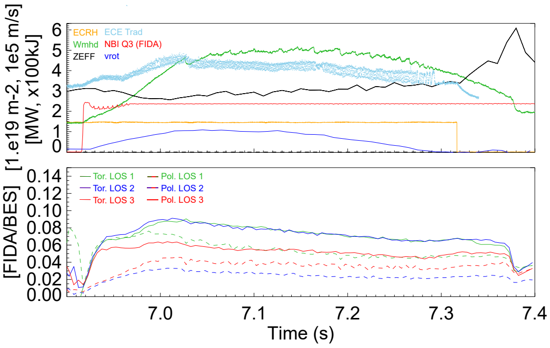

Figure 4: Top: Time trace of AUG shot #41098 showing the slowing down and locking mode around 7.3 s. Bottom: FIDA/BES measurements of three radial locations and two viewing angles.

Simulating the fast ion distribution function as before results in a reasonable match to the measured profile, as can be observed in fig. 6. The FIDASIM simulation based on NUBEAM matches the measurements well over half of the profile. Including a synthetic perturbation in the same way as [6] in the BEAMS3D simulations decreases the simulated values in the core, increasing the match to the data. Adding an artificially high perturbation continues this trend and results in an unreasonably low profile. Figure 5 shows the fast ion density contours together with Poincaré traces of the magnetic field. The shift of the fast ion orbits with respect to the flux surfaces is visible, as well as the perturbation structure, which extends to the core. An island

Figure 5: Poincaré traces (black) and fast ion density contours including perturbations using the normal (left) and an increased (right) magnitude.

structure is visible at R=1.4 m in the fast ion density for the increased perturbation, which is not the case for the normal amplitude one.

This demonstrates the capability to model the effects of an applied magnetic perturbation on the fast ion distribution using BEAMS3D and subsequent comparison to experimental data. Future work will assess these effects in more detail in the presented and additional cases. The validation efforts presented here also give confidence in BEAMS3D for its application to W7-X.

Figure 6: Radial FIDA/BES profiles for the locked mode.

Acknowledgement

This work has been carried out within the framework of the EUROfusion Consortium, funded by the European Union via the Euratom Research and Training Programme (Grant Agreement No 101052200 — EUROfusion). Views and opinions expressed are however those of the author(s) only and do not necessarily reflect those of the European Union or the European Commission. Neither the European Union nor the European Commission can be held responsible for them.

References

[1] M. McMillan, S. Lazerson, 2020 *Plasma Phys. Control. Fusion*, **56** 095019
[2] L.C. Stagner *et al.*, FIDASIM Code *10.5281/zenodo.1341369*
[3] A. Pankin *et al.*, 2004 *Computer Physics Communications*, **159**(3) 157-184
[4] B. Geiger *et al.*, 2020 *Plasma Phys. Control. Fusion*, **62** 105008
[5] R. Fischer *et al.*, 2010 *Fusion Science and Technology*, **58**(2) 675-684
[6] E. Strumberger *et al.*, 2008 *New J. Phys.*, **10**(2) 023017